Universal back-projection algorithm for photoacoustic computed tomography

Minghua Xu, Lihong V. Wang

Minghua Xu, Lihong V. Wang, "Universal back-projection algorithm for photoacoustic computed tomography," Proc. SPIE 5697, Photons Plus Ultrasound: Imaging and Sensing 2005: The Sixth Conference on Biomedical Thermoacoustics, Optoacoustics, and Acousto-optics, (25 April 2005); doi: 10.1117/12.589146

SPIE.

Event: SPIE BiOS, 2005, San Jose, CA, United States

Universal back-projection algorithm for photoacoustic computed tomography

Minghua Xu and Lihong V. Wang*
Optical Imaging Laboratory, Department of Biomedical Engineering
Texas A&M University, 3120 TAMU, College Station, Texas 77843-3120

ABSTRACT

We report a universal back-projection formula for three-dimensional photoacoustic computed tomography in three types of imaging geometries: planar, spherical, and cylindrical surfaces. A solid-angle weighting factor is introduced in the back-projection formula to compensate for the variations of detection views. Numerical simulation demonstrates the performance of the algorithm.

Keywords: Back-projection, algorithm, photoacoustic computed tomography

1. INTRODUCTION

Photoacoustic (PA) computed tomography is based on the reconstruction of an internal PA source distribution from measurements acquired by scanning small-aperture ultrasound detectors over a surface that encloses the source under study [1]. The PA source is produced inside the sample by the thermal expansion that results from a small temperature rise, which is caused by absorption of externally applied radiation of pulsed electromagnetic (EM) waves. This technique has great potential for application in the biomedical field because of the advantages of ultrasonic resolution in combination with EM absorption contrast. In general, different measurement geometries need different reconstruction algorithms. The three geometries commonly used are planar, cylindrical and spherical surfaces. In the last decade, Fourier-domain reconstruction formulas with point-detector measurements for these geometries have been derived (summarized in Ref. [1]), but they may involve multiple integrations or series summations and can be inconvenient to implement. Alternatively, some approximate time-domain back-projection reconstruction algorithms have also been reported [2-4]. In these algorithms, the acoustic property of the tissue is often assumed to be homogenous as the speed of sound in soft tissue is relatively constant at 1.5 mm/ms. The unique advantage of photoacoustic imaging is its ability to detect the inhomogeneous EM absorption property of tissues when the acoustic property is relatively homogeneous. Pure acoustic property differentiation should appeal to conventional ultrasound imaging.

In this paper, we present a universal back-projection (BP) formula, which offers exact reconstructions for the three common geometries and can be easily implemented in the reconstruction. For the spherical geometry, we note that a similar inversion formula was recently reported [5]; however, it can be simplified to the formula that we present here.

2. INVERSE PROBLEM

According to the PA generation theory, the initial photoacoustic pressure at position $\mathbf{r}$ excited by a $\delta(t)$ EM pulse equals $p_0(\mathbf{r}) = \Gamma(\mathbf{r})A(\mathbf{r})$ [6], where $A(\mathbf{r})$ is a spatial EM absorption function and $\Gamma(\mathbf{r})$ is the Grüneisen parameter equal to $c^2\beta/C_p$ (c–the speed of sound; β–the isobaric volume expansion coefficient, and C_p–the specific heat). The acoustic wave, $p(\mathbf{r},t)$ at position $\mathbf{r}$ and time t, prompted by the initial source $p_0(\mathbf{r})$, satisfies the wave equation [6]:

$$(\nabla^2 - \frac{1}{c^2}\frac{\partial^2}{\partial t^2})\, p(\mathbf{r},t) = -p_0(\mathbf{r})\frac{d\delta(t)}{dt}. \qquad (1)$$

* To whom all correspondence should be addressed. Telephone: 979-847-9040; fax: 979-845-4450; electronic mail: LWang@tamu.edu; URL: http://oilab.tamu.edu

Photons Plus Ultrasound: Imaging and Sensing 2005, edited by Alexander A. Oraevsky, Lihong V. Wang, Proceedings of SPIE Vol. 5697 (SPIE, Bellingham, WA, 2005)
1605-7422/05/$15 · doi: 10.1117/12.589146

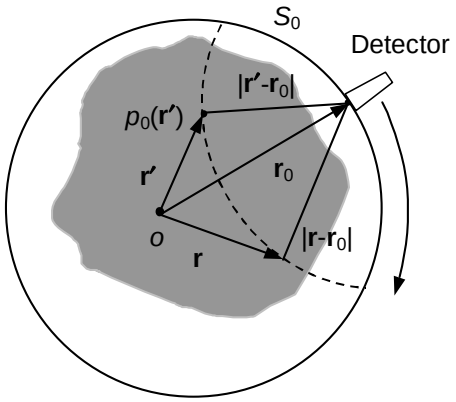

Figure 1: In the measurement, an ultrasonic detector at position $\mathbf{r}_0$ on a surface S_0 receives PA signals emitted from source $p_0(\mathbf{r}')$. In the reconstruction, a quantity related to the measurement at position $\mathbf{r}_0$ projects backward on a spherical surface with respect to position $\mathbf{r}_0$.

As shown in Fig.1, measurement surface S_0 encloses the source $p_0(\mathbf{r}')$. Based on Green's theorem, the pressure $p(\mathbf{r}_0,t)$ detected at $\mathbf{r}_0$ (on S_0) can be written as

$$p(\mathbf{r}_0,t)=\frac{\partial}{\partial t}\left[\frac{t}{4\pi}\int\int_{|\mathbf{r}_0-\mathbf{r}'|=ct}p_0(\mathbf{r}')d\Omega'\right]. \tag{2}$$

where $d\Omega'$ is the solid-angle element of vector $\mathbf{r}'$ with respect to the point at $\mathbf{r}_0$. Now, the problem is to use the measured PA signals $p(\mathbf{r}_0,t)$ to reconstruct the initial source $p_0(\mathbf{r}')$. From a physical point of view, PA tomography (PAT) represents an inverse problem analogous to Positron Emission Tomography (PET), except that PAT is based on diffraction "optics" due to the diffraction of the ultrasonic wave and PET is based on geometric "optics" due to the straight-line propagation of the γ-rays. Therefore, PAT belongs to the field of diffraction tomography. Since acoustic waves do not travel along straight lines, the projections are not line integrals, which are in contrast to those in straight-ray tomography such as PET and x-ray computed tomography (CT). Nevertheless, many imaging concepts and mathematical techniques for other imaging modalities, such as ultrasonic, x-ray and optical tomography, can be borrowed for PAT applications.

3. BACK-PROJECTION FORMULA

In principle, we can construct a Dirichlet Green's function and then write down a form reconstruction formula [7]. For the three common geometries, Dirichlet Green's functions can be written in some explicit expressions [7], with which we can directly write down the reconstruction formulas that are identical to the Fourier-domain formulas summarized in Ref. [1].

Our further study shows that the Fourier-domain reconstruction formulas for the three common geometries can be further simplified into a universal back-projection formula:

$$p_0^{(b)}(\mathbf{r}')=-\frac{2}{\Omega_0}\nabla\cdot\int_{S_0}\mathbf{n}_0^s dS_0\left[\frac{p(\mathbf{r}_0,\bar{t})}{\bar{t}}\right]_{\bar{t}=|\mathbf{r}'-\mathbf{r}_0|}, \tag{3}$$

where Ω_0 is the solid angle of the whole surface S_0 with respect to the reconstruction point inside S_0: $\Omega_0=2\pi$ for the planar geometry and $\Omega_0=4\pi$ for the spherical and cylindrical geometries; $\mathbf{n}_0^s$ is the normal of surface S_0 pointing

to the source. In addition, as mentioned before, a similar inversion formula for the spherical geometry was reported in Ref. [5]. We find it can be simplified to Eq. (3) [7].

Further, we can rewrite Eq (3) in a clear back-projection form as:

$$p_0^{(b)}(\mathbf{r}') = \int_{\Omega_0} b(\mathbf{r}_0, \bar{t} = |\mathbf{r}' - \mathbf{r}_0|) d\Omega_0 / \Omega_0 , \tag{4}$$

where $b(\mathbf{r}_0, \bar{t}) = 2p(\mathbf{r}_0, \bar{t}) - 2\bar{t}\partial p(\mathbf{r}_0, \bar{t})/\partial \bar{t}$ is the back-projection term related to the measurement at position $\mathbf{r}_0$ and

$$d\Omega_0 = \frac{dS_0}{|\mathbf{r}' - \mathbf{r}_0|^2} \cdot \frac{\mathbf{n}_0^s \cdot (\mathbf{r}' - \mathbf{r}_0)}{|\mathbf{r}' - \mathbf{r}_0|}, \tag{5}$$

which is the solid angle for a detection element dS_0 with respect to a reconstruction point P at $\mathbf{r}'$. The term $d\Omega_0/\Omega_0$ is a factor weighting the contribution to the reconstruction from the detection element dS_0. The reconstruction simply projects the quantity $b(\mathbf{r}_0, \bar{t})$ backward on a spherical surface with respect to position $\mathbf{r}_0$. The first derivative over time t actually represents a pure ramp filter k in the frequency domain. The ramp filter depresses the low-frequency signal. It is not surprising that the relatively high-frequency components of the PA signal play the primary role in the reconstruction of the acoustic source inside the tissue.

4. NUMERICAL SIMULATION

We want to use numerical simulation to test the proposed algorithm. For simplicity, we consider uniform spherical absorbers surrounded by a non-absorbing background medium. Without loss of generality, we can take the planar measurement surface as an example.

As shown in Fig. 2, a rectangular-shaped detector: 2 mm × 2 mm, scans the samples in the $z = 0$ plane along both the x-axis and the y-axis from -30 mm to 30 mm with a spatial sampling period of 2/3 mm. Five absorbers are evenly distributed at a distance of 15 mm along the horizontal line ($y = 0$ and $z = 15$ mm) that is parallel to the x-axis; and each absorber has a radius of 1.5 mm and an intensity of 1. Another two absorbers are located at a distance of 15 mm along a horizontal line ($x = 0$ and $z = 15$ mm) that is parallel to the y-axis; and each absorber has a radius of 4 mm and an intensity of 1. Here, we add in the simulated data a Hanning window with temporal cutoff frequency $f_c = 4$ MHz and the data sampling frequency as 20 MHz.

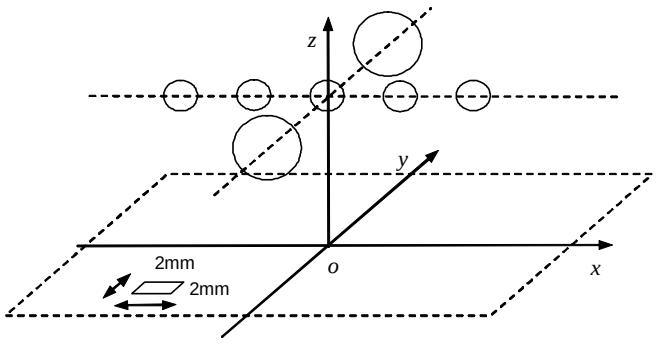

Figure 2: Diagram of planar measurement geometry.

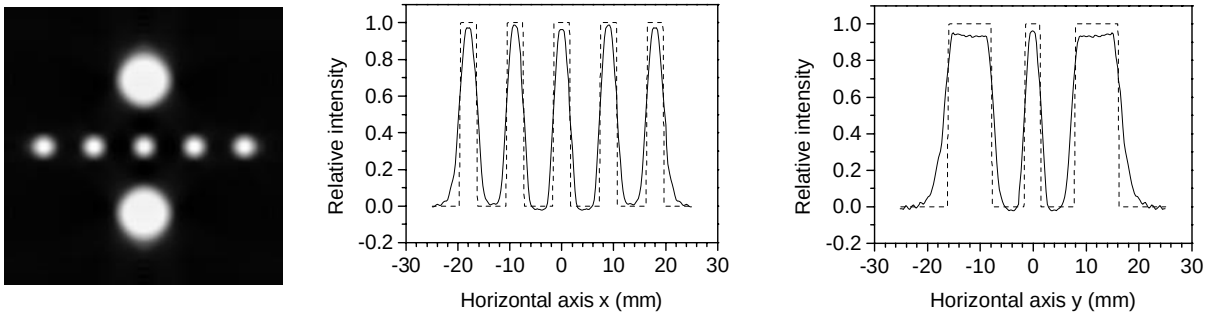

(a) (b) (c)

Figure 3: (a) Grayscale image of the reconstructed pressure distribution in the z = 15 mm plane. Comparison between the original (dashed line) and reconstructed (solid line) distributions: (b) along y = 0 mm and (c) along x = 0 mm.

Figure 3(a) is the grayscale image of the reconstructed distribution in the z = 15 mm plane, and Figs. 3(b) and (c) show the comparison between the original and reconstructed distributions along lines y = 0 and x = 0 mm, respectively. The reconstructed values are in good agreement with the original ones. Due to the limited-angle view and the limited bandwidth, some discrepancies occur in the reconstruction, but they are minimal.

5. SUMMARY

We have presented in this paper a unified and exact time-domain back-projection algorithm for the three common measurement geometries with the assumption of constant sound speed. We can extend this algorithm straightforwardly to the limited-angle view case, in which the reconstruction may be incomplete and reconstruction artifacts may occur. The solid-angle weighting factor in the BP formula, however, can compensate for the variations in the detection views. It has to be pointed out that significant acoustic inhomogeneity of the sample may introduce reconstruction distortions, which, however, may be corrected or minimized using modified algorithms that take account of the acoustic inhomogeneity. This BP formula can serve as the basis for time-domain photoacoustic reconstruction in the three-dimensional space. In principle, this algorithm can also be extended to other inverse-source diffraction tomography

ACKNOWLEDGEMENTS

This project was sponsored in part by the U.S. Army Medical Research and Materiel Command Grant No. DAMD17-00-1-0455, the National Institutes of Health Grants No. R01 EB000712 and No. R01 NS46214, and Texas Higher Education Coordinating Board Grant No. ARP 000512-0063-2001.

REFERENCES

1. M.-H. Xu and L.-H. Wang, Phys. Rev. E 67, 056605, (2003).
2. R. A. Kruger, D. R. Reinecke and G. A. Kruger, Med. Phys. 26, 1832 (1999).
3. M.-H Xu and L.-H. Wang, IEEE Trans. Med. Imaging 21, 814 (2002).
4. M.-H. Xu, Y. Xu, and L.-H. V. Wang, IEEE Trans. Bio-med Eng. 50, 1086 (2003).
5. D. Finch, S. K. Patch, and Rakesh, SIAM J. Math. Anal. 35, 1213 (2003).
6. V. E. Gusev, and A. A. Karabutov, Laser Optoacoustics (AIP, New York, 1993).
7. M.-H. Xu and L.-H. Wang, Phys. Rev. E, in press (2005).